

Teaching Case

Positron Emission Tomography and Magnetic Resonance Imaging Findings in the Diagnosis of Stroke-Like Migraine Attacks after Radiation Therapy Syndrome: A Case Report



Steven D. Pan, MD,^{a,*} Joseph R. Osborne, MD, PhD,^a Gloria C. Chiang, MD,^a Rohan Ramakrishna, MD,^b Apostolos J. Tsiouris, MD,^a Howard A. Fine, MD,^c and Jana Ivanidze, MD, PhD^a

^aDepartment of Radiology, Weill Cornell Medicine, New York, New York; ^bDepartment of Neurosurgery, Weill Cornell Medicine, New York, New York; and ^cDepartment of Neurology, Weill Cornell Medicine, New York, New York

Received 27 December 2023; accepted 13 June 2024

Background

Stroke-like migraine attacks after radiation therapy (SMART) syndrome is a delayed complication of cranial irradiation, associated with migraine-like headaches as well as subacute onset of stroke-like symptoms.¹⁻⁹ Seizure is another common symptom of SMART syndrome, reported in 35% to 83% of cases, and can be either focal or generalized.^{10,11} Although SMART syndrome has been reported in both adult and pediatric populations, the overall incidence is unknown because of its rarity.^{3,8}

18F-Fluorodeoxyglucose (FDG) positron emission tomography (PET) is a widely used diagnostic modality that measures regional glucose metabolism using a radioactive form of glucose.¹²⁻¹⁴ High tissue glucose metabolism, reflected by high FDG avidity, can be due to not only cancer but also infection and inflammation.^{15,16} Despite challenges of physiological high FDG avidity in normal cortical gray matter and deep gray nuclei, FDG PET is often used in brain tumor management to differentiate recurrent tumor and radiation necrosis,¹⁷

especially because FDG is widely available and other more targeted PET radiotracers such as amino acid analogs are currently not U.S. Food and Drug Administration –approved in the United States. FDG PET features in SMART syndrome have not been well characterized, although previous case reports have demonstrated increased cortical FDG avidity in the acute phase of disease.^{2,5} Here, we describe the FDG PET/magnetic resonance imaging (MRI) findings of SMART syndrome in the acute phase as well as longitudinal follow-up evaluation for up to 12 months after presentation.

The clinical and imaging findings of SMART syndrome have long been believed to be an acute manifestation, with cortical enhancement previously described to resolve within 35 days.² We present a case of a 39-year-old woman with anaplastic oligodendroglioma with increased gyriform FDG avidity and corresponding gyriform enhancement on MRI, with the latter persisting for 3 months after presentation. The term “gyriform” refers to a pattern of serpentine enhancement or FDG avidity within the cortex, corresponding to the morphology of the cerebral gyri.¹⁸ In SMART syndrome, this enhancement pattern has been observed on follow-up MRI after radiation therapy and is one of the key imaging features for its diagnosis.^{1,2,19-22} This pattern of enhancement has also been observed in ischemic, epileptic, inflammatory, and neoplastic processes.^{18,23} Through the longitudinal

Sources of support: This work had no specific funding.

All data generated and analyzed during this study are included in this published article.

*Corresponding author: Steven D. Pan, BSc; Email: sdp4002@med.cornell.edu

<https://doi.org/10.1016/j.adro.2024.101567>

2452-1094/Published by Elsevier Inc. on behalf of American Society for Radiation Oncology. This is an open access article under the CC BY-NC-ND license (<http://creativecommons.org/licenses/by-nc-nd/4.0/>).

characterization of MRI findings and the description of PET/MRI characteristics, we aimed to improve the understanding of the clinical features of this rare condition and improve diagnostic accuracy, minimizing the need for invasive procedures such as brain biopsy to differentiate SMART syndrome from recurrent neoplasm.

Case Report

The patient is a 39-year-old woman with a history of left frontal World Health Organization grade 3 anaplastic oligodendroglioma diagnosed 9 years prior to presentation (Fig. 1a, b), status post resection, and 4 cycles of procarbazine, lomustine, and vincristine completed 8 years prior to presentation. Reresection was performed 6 years prior to presentation for tumor recurrence of tumor observed along the anterior resection cavity margin (Fig. 1c, d). The patient also received concurrent external beam radiation therapy and temozolomide, with 13 cycles of adjuvant temozolomide completed 4 years prior to presentation.

Interval history following the last cycle of adjuvant temozolomide had been unremarkable until an episode of speech arrest and arm shaking while on the phone with her son at the time of presentation, with left-sided weakness and left facial droop. The episode lasted for 3 to 5 minutes. Emergency workup included head computed tomography notable for left frontal encephalomalacia (negative for bleeding), blood work (negative for infection), and a loading dose of levetiracetam (1000 mg). The patient had self-discontinued her recommended regimen of levetiracetam (1000 mg daily) >1 year ago because of headaches after taking the medication. The patient was restarted on levetiracetam (500 mg every 12 hours) and advised for follow-up PET/MRI to evaluate for tumor recurrence as a possible etiology of seizure.

In addition to epilepsy secondary to tumor recurrence and progression of disease, the differential diagnostic considerations also included a primary cerebrovascular event not detected on initial computed tomography imaging, in addition to the possibility of peri-ictal pseudoprogression, in which patients experience epileptic seizures or seizure-like symptoms without true progression of neoplastic disease.²⁴

The patient's last prior normal follow-up imaging was performed 8 months prior to presentation and demonstrated stable confluent pericavitary T2 fluid-attenuated inversion recovery (FLAIR) hyperintensity, favored to represent posttreatment changes (Fig. 1e, f). Subsequent follow-up MRI performed at 1 month after presentation demonstrated significant gyriform enhancement along the anterolateral resection cavity of the left frontal lobe, observed on both T1 postcontrast and T2 FLAIR sequences (Fig. 2b, c). Dynamic contrast-enhanced MRI perfusion imaging demonstrated mild-

to-moderate associated plasma volume elevation along the resection cavity; there was corresponding reduced diffusion (Fig. 2d-f).

Concurrently performed FDG PET/MRI demonstrated markedly increased FDG avidity corresponding to the area of gyriform enhancement visualized on MRI, with a standardized uptake value (SUV) of 31.6 in the area of focal avidity compared with an SUV of 16.7 in the normal-appearing right frontal cortex and an SUV of 5.2 in normal-appearing right parietal white matter (Fig. 3). Thus, the pattern of intense FDG avidity followed the characteristic gyriform enhancement pattern visualized on MRI.

Overall, the gyriform left frontal enhancement with corresponding T2 hyperintensity and intense FDG avidity in the clinical setting of seizure-like presentation with a prior history of radiation therapy favored the diagnosis of SMART syndrome. Management included active MRI surveillance with brain biopsy deferred pending imaging findings.

While follow-up imaging at 2 months after presentation showed no changes in gyriform enhancement, follow-up MRI at 3 months after presentation showed significant interval decrease in left frontal gyriform enhancement and no new intracranial enhancement (Fig. 4c, d) in the absence of any treatment. There was decreased cortical T2 hyperintensity and no associated reduced diffusion or intrinsic T1 shortening compared with prior imaging performed at 1 month after presentation (Fig. 4a-d). Given the marked decrease in enhancement without treatment and the absence of interval clinical history and findings, a definitive diagnosis of SMART syndrome was made. Additional 5-month follow-up on MRI demonstrated complete resolution of initial enhancement (Fig. 4e, f).

While follow-up postcontrast T1 imaging at 3 months and 5 months after presentation demonstrated significant regression of the gyriform enhancement (Fig. 4c-f), longitudinal MRI also demonstrated persistence of marginal enhancement along posterior enhancement at 12 months after presentation (Fig. 5a). In addition, T2 FLAIR imaging demonstrated evolving enhancement at the posterior resection cavity margin (Fig. 4e, f), also raising the suspicion of viable tumor in the background of posttreatment changes. Thus, repeat FDG PET/MRI was performed at 12 months after presentation, which demonstrated lack of FDG avidity associated with this focus of enhancement along the posterior cavity margin (Fig. 5b). FDG PET/MRI also demonstrated resolution of the gyriform avidity previously visualized on initial FDG PET/MRI (Fig. 5b). Repeat FDG PET/MRI further suggested evolving post-radiation treatment-related changes rather than tumor recurrence. In addition, during subsequent clinical follow-up, the patient did not report any recurrence of the symptoms that had led to her initial presentation to the emergency department.

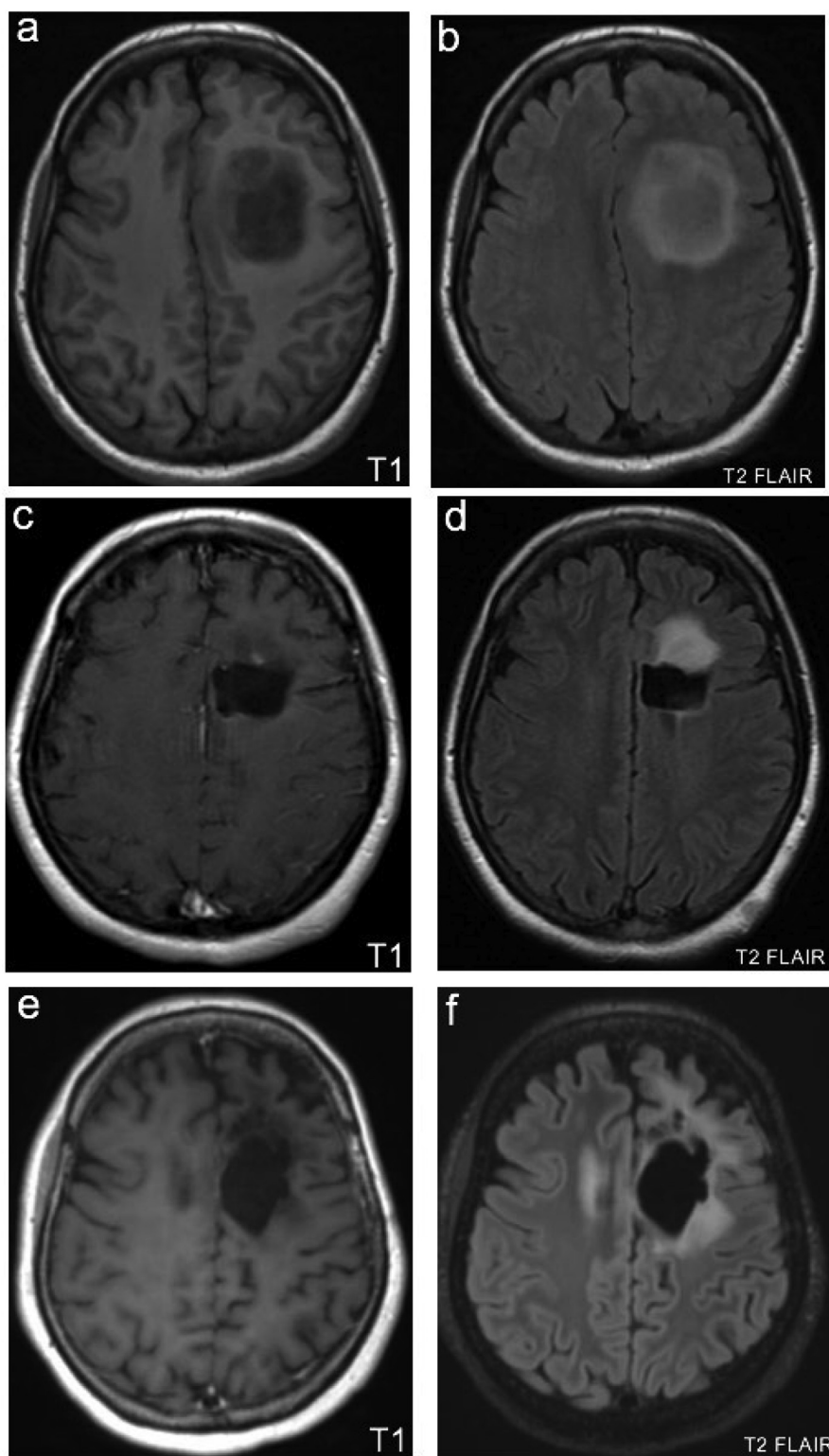


Figure 1 Magnetic resonance imaging findings prior to symptomatic presentation. (a) T1 and (b) T2 fluid-attenuated inversion recovery (FLAIR) images prior to resection (9 years prior to current presentation). Large mass corresponding to tumor in the left frontal lobe, with mass effect on the left lateral ventricle, compatible with initial diagnosis of anaplastic oligodendroglioma. (c) T1 and (d) T2 FLAIR images corresponding to tumor recurrence (6 years prior to current presentation) following initial resection. An area of abnormal enhancement along the anterior resection cavity was observed on T2 imaging, corresponding to recurrent disease. (e) Postcontrast T1 and (f) T2 FLAIR imaging of the most recent follow-up scan following reresection of tumor (8 months prior to presentation) showing no suspicious enhancement with unchanged extent of confluent pericavitary T2 hyperintensity involving the right centrum semiovale and left corona radiata. Imaging is favored to represent treatment-related change.

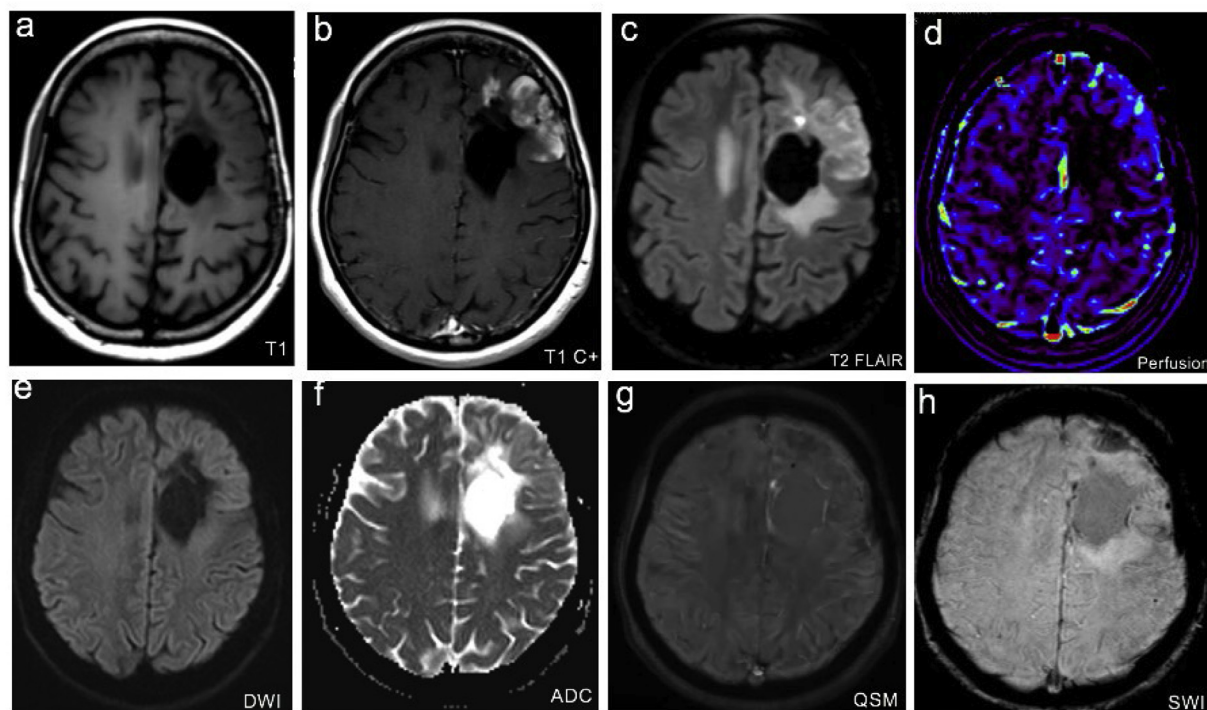


Figure 2 Magnetic resonance imaging findings 1 month after symptomatic presentation. (a) No associated precontrast T1 shortening. Increased gyriform enhancement along the anterolateral resection cavity margin on both (b) T1 postcontrast and (c) T2 fluid-attenuated inversion recovery (FLAIR) imaging. (d) Dynamic contrast-enhanced perfusion demonstrates mild-to-moderate associated plasma elevation along the resection cavity (plasma volume (VP) up to 0.06 compared with contralateral VP 0.01 in normal brain). (e) Mildly reduced diffusion along the anterior and medial resection cavity margins, extending along the cortices of the left superior and middle frontal gyri and into the left frontal operculum and (f) corresponding mild hypointensity on the apparent diffusion coefficient (ADC) map along the anterior and medial resection cavity. (g) Region of curvilinear hyperintensity along the resection cavity observed in quantitative susceptibility mapping (QSM) as well as (h) corresponding region of curvilinear hypointensity observed on susceptibility-weighted imaging (SWI) suggestive of pericavitary hemosiderin staining. *Abbreviation:* DWI: diffusion-weighted imaging.

Discussion

Pseudoprogression, radiographically defined as transient imaging findings suggestive of possible tumor progression and typically 3 to 6 months after radiation therapy, can also present with symptoms such as headache, seizures, and focal neurologic deficits, making clinical differentiation from true tumor progression challenging.^{25,26} While FDG is the most widely used PET radiotracer for functional evaluation of brain lesions, the use of FDG PET to distinguish radiation necrosis from recurrent tumor has produced mixed results,²⁵ with some studies reporting high accuracy while others report low sensitivity and specificity.²⁶⁻²⁹ The use of FDG PET in diagnosing SMART syndrome has not been well characterized, and given its high cortical FDG avidity observed on PET imaging, it may be difficult to differentiate SMART syndrome from neoplastic, infectious etiologies.^{1,2,30} However, as seen in our patient's imaging, the metabolic activity on PET also demonstrates a unique, gyriform enhancement pattern, similar to the enhancement pattern visualized on MRI. Thus, when using FDG

PET in the diagnosis of SMART syndrome, the recognition of its unique, cortical gyriform pattern of hypermetabolism is crucial in the accurate diagnosis of this disease.

Although MRI alone may be able to diagnose SMART syndrome, the imaging findings from this case demonstrate the utility of FDG PET as an adjunct diagnostic tool. The radiographic differentiation between progression and post-radiation therapy pseudoprogression remains a diagnostic challenge in the post-radiation therapy setting.³¹ While both viable tumor and pseudoprogression demonstrate contrast enhancement on MRI imaging, features such as focal nodular enhancement, subependymal enhancement, or larger extent of T2 FLAIR signal abnormality generally favor the diagnosis of true neoplastic progression of disease.³²⁻³⁵ In our patient, the imaging findings demonstrate both gyriform enhancement atypical of disease progression as well as extensive T2 FLAIR enhancement, which can be seen in both the context of viable tumor and pseudoprogression. FDG PET can be an adjunct imaging modality in the diagnosis of progression of disease versus post-radiation therapy change for patients with primary glioma neoplasms, and

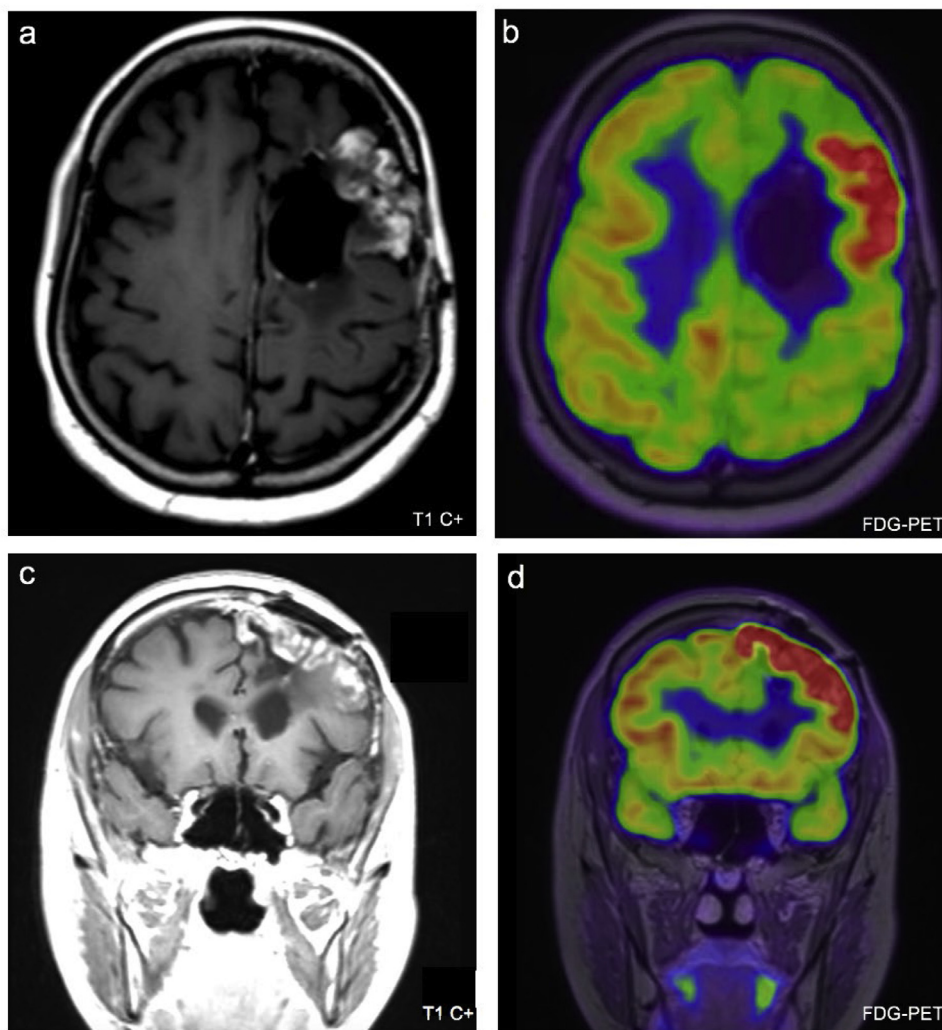


Figure 3 18F-Fluorodeoxyglucose (FDG) positron emission tomography (PET) findings 1 month after symptomatic presentation. PET windowed to 0 to 15. Axial view of (a) T1 postcontrast and (b) fused FDG PET and magnetic resonance imaging obtained at 1 month after initial emergency department presentation. FDG PET demonstrates gyri-form intense avidity with a standardized uptake value of 31.6 corresponding to the area of left frontal cortical enhancement. This is further illustrated on coronal views demonstrating gyri-form enhancement along the left frontal cortex was also observed in the coronal view on (c) T1 postcontrast imaging and (d) fused PET/magnetic resonance imaging windowed to a standardized uptake value of 0 to 15.

the pattern of gyri-form FDG avidity has not been observed in cases of viable tumor on PET imaging.^{31,36-38} Thus, in cases where initial MRI demonstrates findings that raise the possibility for both pseudoprogression and progression of disease, FDG PET may serve as an important tool in the diagnosis of SMART syndrome. Furthermore, because enhancement on MRI can persist for several months, as demonstrated by this case of SMART syndrome, an immediate FDG PET can serve to diagnose pseudoprogression prior to the findings on sequential MRIs demonstrating resolution of enhancement, advancing patient management in a timelier manner.

When there is a persistent component of enhancement visualized on longitudinal MRI, as in this case with T1 postcontrast, longitudinal FDG PET may also serve to determine whether there is a component of viable tumor

in the setting of evolving post-radiation therapy treatment-related changes. In this case, repeat FDG PET at 12 months after presentation demonstrated no corresponding avidity to the enhancement on T1 postcontrast imaging (Fig. 5a, b), further suggesting post-radiation therapy treatment-related changes instead of true tumor progression. Thus, for any cases of SMART syndrome that continue to demonstrate findings raising the possibility of viable neoplasm on follow-up MRI imaging, longitudinal FDG PET may also play an additional role in ruling out progression of disease.

When considering additional differential diagnoses, epilepsy also demonstrates a similar cortical gyri-form avidity on FDG PET.³⁹⁻⁴¹ While seizure is not the most common clinical manifestation of SMART syndrome, it has been reported in many cases.^{10,11} Previous studies

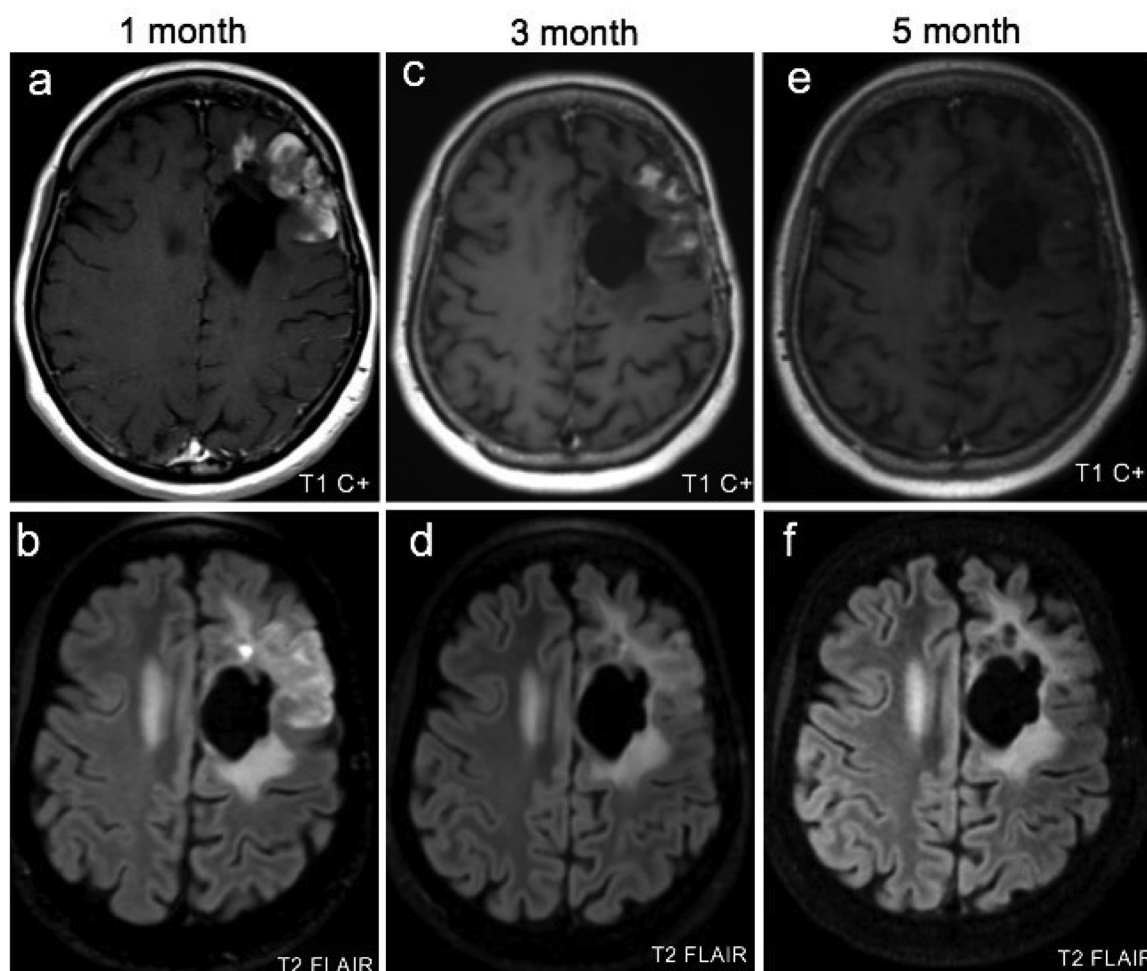


Figure 4 Longitudinal magnetic resonance imaging findings following initial symptomatic presentation. (a, b) T1 postcontrast and T2 fluid-attenuated inversion recovery (FLAIR) images obtained at 1 month after presentation. (c, d) T1 postcontrast and T2 FLAIR images obtained at 3 months after presentation. (e, f) T1 postcontrast and T2 FLAIR images obtained at 5 months following the emergency department presentation. Continued decrease in heterogeneous gyriiform enhancement and T2 FLAIR intensity over a 5-month period without any additional intervention. Temporal evolution in gyriiform enhancement pattern suggests a self-limiting process such as stroke-like migraine attacks after radiation therapy syndrome as the underlying cause of imaging findings.

examining the use of FDG PET in epilepsy patients showed the highest sensitivity of these imaging findings in the ictal and postictal states⁴² immediately following the episode of epilepsy. Thus, the presence of FDG avidity 1 month following initial presentation of symptoms demonstrates the additional utility of FDG PET for differentiating SMART syndrome from the diagnosis of epilepsy.

Previously, the findings of hypermetabolism on FDG PET were only reported up to 4 days after the initial episode of symptoms,³⁰ but the persistence of FDG avidity 1 month following symptomatic presentation highlights a longer time course in both the development and resolution of characteristic imaging findings.

Brain MRI is currently the primary imaging technique of choice, demonstrating unilateral cortical enhancement on T2 and FLAIR sequences.^{2-5,8} These imaging findings have previously been reported to develop within 2 to 7 days of symptomatic presentation and resolve within 13

to 35 days.² This case demonstrates the persistence of cortical enhancement on MRI at 3 months after presentation, with resolution of imaging findings only at 5 months after presentation. Thus, when determining follow-up imaging, recognition of a gradual attenuation of enhancement rather than quicker resolution than previously described is critical in the diagnosis of SMART syndrome and differentiation from acute processes like epilepsy and infection or progressive disorders like neoplasm.

Although SMART syndrome is most commonly self-resolving with transient symptoms, there have been cases of recurrent SMART syndrome reported, with seizure-like symptoms returning 6 weeks following initial presentation.^{20,43} While enhancement observed on MRI at 3 months after presentation represents a novel length in the persistence of imaging findings for SMART syndrome,^{2,6,7,43} the patient reported no recurrence of symptoms following her initial presentation to the

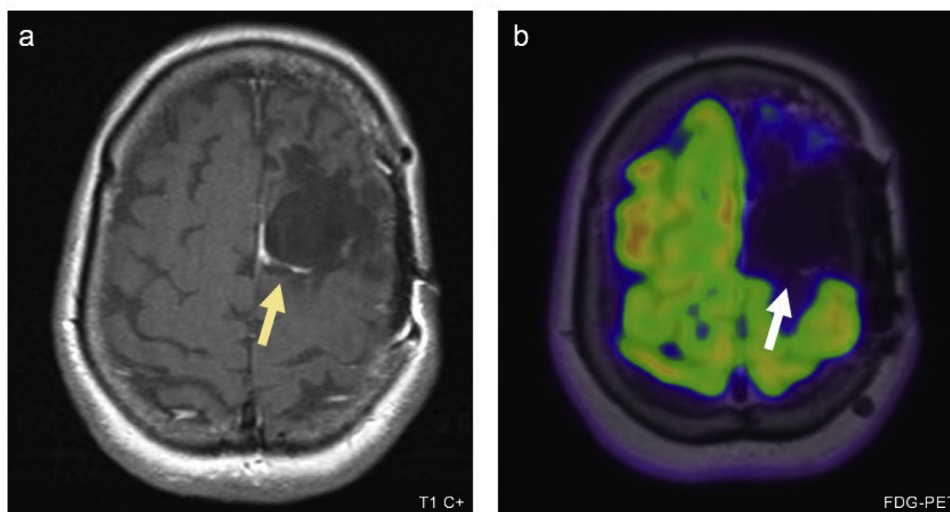


Figure 5 18F-Fluorodeoxyglucose (FDG) positron emission tomography (PET) findings 12 months after symptomatic presentation. (a) T1 postcontrast magnetic resonance imaging (MRI) at 12 months after presentation demonstrating resolution of cortical gyriform enhancement. There is a slightly increased curvilinear enhancement along the posterior resection cavity (yellow arrow). (b) Concurrently performed FDG PET/MRI demonstrating no associated FDG avidity (white arrow), supporting evolving post-treatment changes rather than viable tumor. Fused FDG PET/MRI images windowed to a standardized uptake value of 0 to 15.

emergency department, suggesting that the duration of imaging findings diagnostic of SMART syndrome may exceed clinical symptom duration.

Conclusion

While an extremely rare complication, imaging has proven crucial to the clinical workup for SMART syndrome.⁵ Through establishing a longitudinal characterization of imaging findings on MRI, as well as the appearance of SMART syndrome on FDG PET/MRI, this report aimed to enhance the understanding of its time course and manifestations in diagnostic imaging, as well as validate the utility of FDG PET imaging in differentiating SMART syndrome from alternative diagnoses such as tumor recurrence or epilepsy. Through improved diagnostic understanding of pseudoprogression manifestations such as SMART syndrome, fewer invasive procedures like brain biopsies will be needed in the future in order to rule out recurrent neoplasm.

Disclosures

None.

References

- Black DF, Bartleson JD, Bell ML, Lachance DH. SMART: stroke-like migraine attacks after radiation therapy. *Cephalalgia*. 2006;26:1137-1142.
- Black DF, Morris JM, Lindell EP, et al. Stroke-like migraine attacks after radiation therapy (SMART) syndrome is not always completely reversible: A case series. *AJNR Am J Neuroradiol*. 2013;34:2298-2303.
- Dominguez M, Malani R. Stroke-like migraine attacks after radiation therapy (smart) syndrome: A comprehensive review. *Curr Pain Headache Rep*. 2021;25:33.
- Ota Y, Leung D, Lin E, et al. Prognostic factors of stroke-like migraine attacks after radiation therapy (SMART) syndrome. *AJNR Am J Neuroradiol*. 2022;43:396-401.
- Ota Y, Liao E, Shah G, Srinivasan A, Capizzano AA. Comprehensive update and review of clinical and imaging features of SMART syndrome. *AJNR Am J Neuroradiol*. 2023;44:626-633.
- Rigamonti A, Lauria G, Mantero V, Filizzolo M, Salmaggi A. SMART (stroke-like migraine attack after radiation therapy) syndrome: A case report with review of the literature. *Neurol Sci*. 2016;37:157-161.
- Singh TD, Hajeb M, Rabinstein AA, et al. SMART syndrome: Retrospective review of a rare delayed complication of radiation. *Eur J Neurol*. 2021;28:1316-1323.
- Zheng Q, Yang L, Tan LM, Qin LX, Wang CY, Zhang HN. Stroke-like migraine attacks after radiation therapy syndrome. *Chin Med J (Engl)*. 2015;128:2097-2101.
- Turnquist C, Harris BT, Harris CC. Radiation-induced brain injury: Current concepts and therapeutic strategies targeting neuroinflammation. *Neurooncol Adv*. 2020;2:vdaa057.
- Di Stefano AL, Berzero G, Ducray F, et al. Stroke-like events after brain radiotherapy: A large series with long-term follow-up. *Eur J Neurol*. 2019;26:639-650.
- Fan EP, Heiber G, Gerard EE, Schuele S. Stroke-like migraine attacks after radiation therapy: A misnomer? *Epilepsia*. 2018;59:259-268.
- Torigian DA, Zaidi H, Kwee TC, et al. PET/MR imaging: Technical aspects and potential clinical applications. *Radiology*. 2013;267:26-44.
- Kwee TC, Basu S, Saboury B, Alavi A, Torigian DA. Functional oncoimaging techniques with potential clinical applications. *Front Biosci (Elite Ed)*. 2012;4:1081-1096.
- Kelloff GJ, Hoffman JM, Johnson B, et al. Progress and promise of FDG-PET imaging for cancer patient management and oncologic drug development. *Clin Cancer Res*. 2005;11:2785-2808.
- Voigt W. Advanced PET imaging in oncology: Status and developments with current and future relevance to lung cancer care. *Curr Opin Oncol*. 2018;30:77-83.

16. Vaidyanathan S, Patel CN, Scarsbrook AF, Chowdhury FU. FDG PET/CT in infection and inflammation—Current and emerging clinical applications. *Clin Radiol*. 2015;70:787-800.
17. Hustinx R, Pourdehnad M, Kaschten B, Alavi A. PET imaging for differentiating recurrent brain tumor from radiation necrosis. *Radiol Clin North Am*. 2005;43:35-47.
18. Smirniotopoulos JG, Murphy FM, Rushing EJ, Rees JH, Schroeder JW. Patterns of contrast enhancement in the brain and meninges. *Radiographics*. 2007;27:525-551.
19. Angelidis P, Saleh C, Jaszczuk P, Seyam M, Ebner KA, Hund-Georgiadis M. SMART syndrome (stroke-like migraine attacks after radiation therapy): When to suspect it? *Surg Neurol Int*. 2021;12:561.
20. April D, Lall N, Steven A. Stroke-like migraine attacks after radiation therapy syndrome. *Ochsner J*. 2020;20:6-9.
21. Armstrong AE, Gillan E, DiMario Jr FJ. SMART syndrome (stroke-like migraine attacks after radiation therapy) in adult and pediatric patients. *J Child Neurol*. 2014;29:336-341.
22. Biju RD, Dower A, Moon BG, Gan P. SMART (stroke-like migraine attacks after radiation therapy) syndrome: A case study with imaging supporting the theory of vascular dysfunction. *Am J Case Rep*. 2020;21: e921795.
23. Silverstein AM, Alexander JA. Acute postictal cerebral imaging. *AJNR Am J Neuroradiol*. 1998;19:1485-1488.
24. Rheims S, Ricard D, van den Bent M, et al. Peri-ictal pseudoprogression in patients with brain tumor. *Neuro Oncol*. 2011;13:775-782.
25. Chao ST, Suh JH, Raja S, Lee SY, Barnett G. The sensitivity and specificity of FDG PET in distinguishing recurrent brain tumor from radionecrosis in patients treated with stereotactic radiosurgery. *Int J Cancer*. 2001;96:191-197.
26. Graeb DA, Steinbok P, Robertson WD. Transient early computed tomographic changes mimicking tumor progression after brain tumor irradiation. *Radiology*. 1982;144:813-817.
27. Kim EE, Chung SK, Haynie TP, et al. Differentiation of residual or recurrent tumors from post-treatment changes with F-18 FDG PET. *Radiographics*. 1992;12:269-279.
28. Thompson TP, Lunsford LD, Kondziolka D. Distinguishing recurrent tumor and radiation necrosis with positron emission tomography versus stereotactic biopsy. *Stereotact Funct Neurosurg*. 1999; 73:9-14.
29. Griffith LK, Rich KM, Dehdashti F, et al. Brain metastases from non-central nervous system tumors: Evaluation with PET. *Radiology*. 1993;186:37-44.
30. Bund C, Fahrner P, Gebus O, Kremer S, Blondet C, Namer IJ. Sequential FDG PET and MRI findings in a case of SMART syndrome. *Seizure*. 2017;51:50-51.
31. Qin D, Yang G, Jing H, Tan Y, Zhao B, Zhang H. Tumor progression and treatment-related changes: Radiological diagnosis challenges for the evaluation of post treated glioma. *Cancers (Basel)*. 2022;14:3771.
32. Reddy K, Westerly D, Chen C. MRI patterns of T1 enhancing radiation necrosis versus tumour recurrence in high-grade gliomas. *J Med Imaging Radiat Oncol*. 2013;57:349-355.
33. Young RJ, Gupta A, Shah AD, et al. Potential utility of conventional MRI signs in diagnosing pseudoprogression in glioblastoma. *Neurology*. 2011;76:1918-1924.
34. Yoo RE, Choi SH, Kim TM, et al. Independent poor prognostic factors for true progression after radiation therapy and concomitant temozolomide in patients with glioblastoma: Subependymal enhancement and low ADC value. *AJNR Am J Neuroradiol*. 2015; 36:1846-1852.
35. Agarwal A, Kumar S, Narang J, et al. Morphologic MRI features, diffusion tensor imaging and radiation dosimetric analysis to differentiate pseudo-progression from early tumor progression. *J Neurooncol*. 2013;112:413-420.
36. Quartuccio N, Laudicella R, Vento A, et al. The additional value of ¹⁸F-FDG PET and MRI in patients with glioma: A review of the literature from 2015 to 2020. *Diagnostics (Basel)*. 2020; 10:357.
37. Takahashi M, Soma T, Mukasa A, Tanaka S, Yanagisawa S, Momose T. Pattern of FDG and MET distribution in high- and low-grade gliomas on PET images. *Clin Nucl Med*. 2019;44:265-271.
38. Parvez K, Parvez A, Zadeh G. The diagnosis and treatment of pseudoprogression, radiation necrosis and brain tumor recurrence. *Int J Mol Sci*. 2014;15:11832-11846.
39. Sone D, Maikusa N, Sato N, Kimura Y, Ota M, Matsuda H. Similar and differing distributions between ¹⁸F-FDG-PET and arterial spin labeling imaging in temporal lobe epilepsy. *Front Neurol*. 2019; 10:318.
40. la Fougère C, Rominger A, Förster S, Geisler J, Bartenstein P. PET and SPECT in epilepsy: A critical review. *Epilepsy Behav*. 2009; 15:50-55.
41. Guedj E, Bonini F, Gavaret M, et al. 18FDG-PET in different subtypes of temporal lobe epilepsy: SEEG validation and predictive value. *Epilepsia*. 2015;56:414-421.
42. Devous Sr MD, Thisted RA, Morgan GF, Leroy RF, Rowe CC. SPECT brain imaging in epilepsy: A meta-analysis. *J Nucl Med*. 1998;39:285-293.
43. Ramanathan RS, Sreedher G, Malhotra K, et al. Unusual case of recurrent SMART (stroke-like migraine attacks after radiation therapy) syndrome. *Ann Indian Acad Neurol*. 2016;19:399-401.